Part-Load Simulation of Combined Cycle and Gas Turbine Power Plants Using DWSIM

Twana N. Hassan, Saif T. Manji and Ahmed A. Maaroof†

Department of Chemical Engineering, Faculty of Engineering, Koya University,
Danielle Mitterrand Boulevard, Koya KOY45, Kurdistan Region – F.R. Iraq

***Abstract*—In Iraq, combined cycle gas turbine (CCGT) systems are the only and main process for power generation (electricity). Due to its importance and significance, accurate simulation is crucial for evaluating the process performance under different operation conditions. In this study, DWSIM software, open-source simulation tool, was used for modeling and assessing CCGT performance during part-load circumstances. This software used for its reliability in capturing operational behavior. The methodology consists of simulating CCGT response under the variation of the power by integrating part-load performance equations into DWSIM software. Generally, two cases included in this work; the first case covered a DWSIM simulation during part-load operation using data from previously published works that used Aspen HYSYS. On the other hand, the second case included performing a DWISM simulation using real filed data. The results gained were validated by comparing it with Aspen HYSYS simulation. The comparison between DWSIM and HYSYS showed a 3.8% variation in power generation, a close match in fuel flow, and a maximum variation of 4.36% in gas turbine efficiency. The findings of this work confirm that the DWSIM software is flexible, free, and reliable simulation tool for evaluating CCGT power plant's performance and operation. In addition, this work presented that this software is suitable for use in both industrial and academic applications due to its performance compared to that of commercial simulators.**

***Index Terms*—Combined cycle, DWSIM, Gas turbine, Part-load operation, Plant load.**

I. Introduction

Worldwide, the primary method for producing electricity and meeting the increasing need for power is combined cycle gas turbine (CCGT) technology (Ibrahim, et al., 2017; Ohanu, Rufai and Oluchi, 2024; Pan et al., 2016). This kind of cycle (CCGT) in power generation consists of two thermodynamic cycles within the same system. Simulation, on the other hand, is the process of replicating a real phenomenon utilizing mathematical equations and correlations. Simulations are often used to test new hypotheses and assess systems performance under different operating conditions (Zabre, et al., 2009). The main components of a CCGT plant are; gas turbine (GT) cycle which includes compressor, combustion chamber and expander and steam cycle which contains heat recovery steam generator (HRSG), steam turbine (ST), air-cooled condenser, and feed water pumps (Bass, et al., 2011; Emenike, Anyaoha and Okoroigwe, 2025; Hussein and İbrahim, 2024; Ravelli, 2025; Xezonakis, Samuel and Enweremadu, 2024).

According to the Brayton cycle, the GT process cycle begins with ambient air entering through the filter house, which removes dust and particulate matter. The air then passes into the axial compressor, which maintains the necessary airflow for turbine cooling and bearing sealing. As a result of adiabatic compression, the air exits the compressor at high pressure (HP) and elevated temperature. This conditioned air is mixed with fuel and injected through a diffuser or nozzle into the combustion chamber, where combustion occurs, raising the temperature to approximately 900–1400°C (Jeffs, 2008; Najjar and Akyurt, 1994). The resulting high-temperature and pressure gases expand through the turbine, where their thermal energy is converted into mechanical energy, and subsequently into electrical power via the generator. The flue gases leaving the exhaust system typically have a temperature of around 560°C (Asadi, et al., 2022; Boles and Cengel, 2014; Boyaghchi, Chavoshi and Sabeti, 2015). Following the Rankine cycle, the waste heat from the GT plant exhaust is recovered in the HRSG, where it is used to produce high-temperature and high-pressure steam in the heat exchangers and steam drums. This steam is used to run a ST, converting the steam's thermal energy into mechanical energy and electricity at the end. This combined cycle configuration greatly improves thermal efficiency, increasing the overall plant efficiency to 60% or more (Glazar, Mrzljak and Gubic, 2019; Khan, et al., 2024; Xu, et al., 2024).

Recent developments in software for simulation of chemical engineering have fundamentally changed the practice of engineering by allowing analysis and optimization of complicated processes that are safe, more economic, and more efficient. Process simulation enables engineers to analyze various operating conditions without conducting

ARO-The Scientific Journal of Koya University
Vol. XIV, No.2 (2026), Article ID: ARO.12620.12 pages
DOI: 10.14500/aro.12620
Received: 15 September 2025; Accepted: 11 May 2026
Regular research paper; Published: 14 June 2026
†Corresponding author's e-mail: ahmed.maaroof@koyauniversity.org

physical experimentation, leading to less operational risk and waste of cost and material. Through the consideration of alternative cases, a high systematic evaluation may be provided, helping potential improvement of processes in terms of being energy efficient and waste minimized (Diddi and Panda, 2024; Kong, et al., 2024) At a technical level, these tools help designers and operators to prove that a process meets safety, environmental, or regulatory conditions. In addition, simulation software helps to observe process activity before and during use as a springboard for understanding system dynamics without real operational hazards (Csendes et al., 2023). This is a necessity for all engineers but also students who want to understand the nature of processes, and how different variables are interacting (Boles and Cengel, 2014; Sadeghi and Ahmadi, 2021).

Within the power generation sector, extensive research has been conducted on the modeling and simulation of CCGT power plants (Leisen, Radek and Weber, 2024; Lu, et al., 2024). Dev, et al. (2012) proposed a mathematical modeling approach based on steam and GT cycle data to evaluate CCGT performance under varying environmental conditions. Their MATLAB-based model assessed power output, efficiency, and electricity generation. Similarly, Can Gülen and Kim (2014) introduced a simplified physics-based method for simulating the dynamic response of the steam bottoming cycle in CCGT plants, focusing on transient efficiency during startup, shutdown, and load variations while maintaining computational efficiency and model transparency.

Other work in CCGT modeling is the approach of Meegahapola and Flynn (2014), which developed a detailed CCGT model in the DIgSILENT dynamic simulation language. They studied the model setup, the impact of ambient conditions, and the stability of system in the presence of energy perturbations. Ibrahim and Rahman (2015) developed a MATLAB model for the IHGT process in a CCGT plant and validated it using real plant data. In parallel, Pal et al. (2015) used the PROSIM software to simulate the thermodynamics of the Rya CHP in combined heat and power mode, which proved to represent key components in a power plant, such as heat exchangers and GTs quite accurately.

Owing to the growing demand for operational flexibility, dynamic and part-load simulation have drawn much attention in many studies. Li, et al. (2017) developed a dynamic simulation model of a 420 MW CCGT power plant using Aspen Plus, incorporating thermal energy storage to enhance operational management through charging and discharging strategies. Encabo Caceres, Mocholí Montañés and Nord, (2018) utilized EBSILON Professional to simulate both full-load and part-load operation of a CCGT power station, examining the economic and performance impacts of supplementary firing and ambient conditions. Liu and Karimi (2018b) proposed a simulation-based optimization strategy for improving CCGT performance during part-load operation through optimized fuel flow control and inlet guide vane (IGV) regulation.

Commercial and open-source simulation tools are being increasingly used in recent studies. Pattanayak, Padhi and Gajjar (2021) studied individual components of a combined cycle power plant using EBSILON in order to investigate an extensive range of operation conditions. Talah, Bentarzi and Mangola (2023) used the Modelica environment to simulate the Ras-Djinet CCGT power plant with decreased fuel flow and turbine inlet temperature, aiming to study operating performance parameters of GTs.

Open-source simulation platforms such as DWSIM have, in recent years, been rising more and more interest for simulating complex energy systems under real operating conditions. Use of DWSIM has shown a promising capability to simulate GTs and combined cycle power plants, especially part-load. DWSIM allows for a more accurate comparison of the operational boundaries and system flexibility as opposed to conventional thermodynamic calculation methods. The capability of DWSIM for academic and industrial purposes (in particular, performance analysis comparison and load following strategy development) has emerged in the recent works published between 2024 and 2025. It is an appealing tool for modelling and optimization of modern power plants due to its flexibility, robustness, and the possibility of detailed investigation of efficiency at part-load (Ali Motamed, Genrup and Nord, 2024; Hashim, Hasan and Al Jubori, 2025; Leisen, Radek and Weber, 2024; Xie, et al., 2024).

Due to the limited accessibility and high cost of commercial simulation tools, this study aims to employ the open-source DWSIM software to simulate a CCGT power plant under part-load operating conditions. The simulation framework includes a comparative assessment between DWSIM and Aspen HYSYS based on previous studies, as well as the validation of the DWSIM model using actual plant operating data.

II. Methodology

CCGTs are complex systems that include various unit operations, advanced thermodynamic cycles, and complicated piping designs. In process and power engineering, simulating CCGTs is considered one of the greatest challenges as it needs specialized knowledge, high level of technical focus, and high level of expertise to produce accurate results. The simplified block flow diagram of CCGT is shown in Fig. 1.

The operation of such a system was found to be significantly affected by external and internal factors such as continuously changing atmospheric temperatures and the demand for power across the seasons. These variations directly affect the performance of the CCGTs, including fuel consumption, efficiency, and electricity generation. These factors increase the demand for producing accurate modeling and real-time operation. Therefore, operators and engineers need to possess a high degree of adaptability, awareness, and skills to guarantee efficient, safe, and stable operation during dynamic circumstances.

CCGT simulation during part-load operation or design is considered one of the most challenging tasks, due to the complexity of the process, which includes multiple unit operations and many interdependent variables. To make the

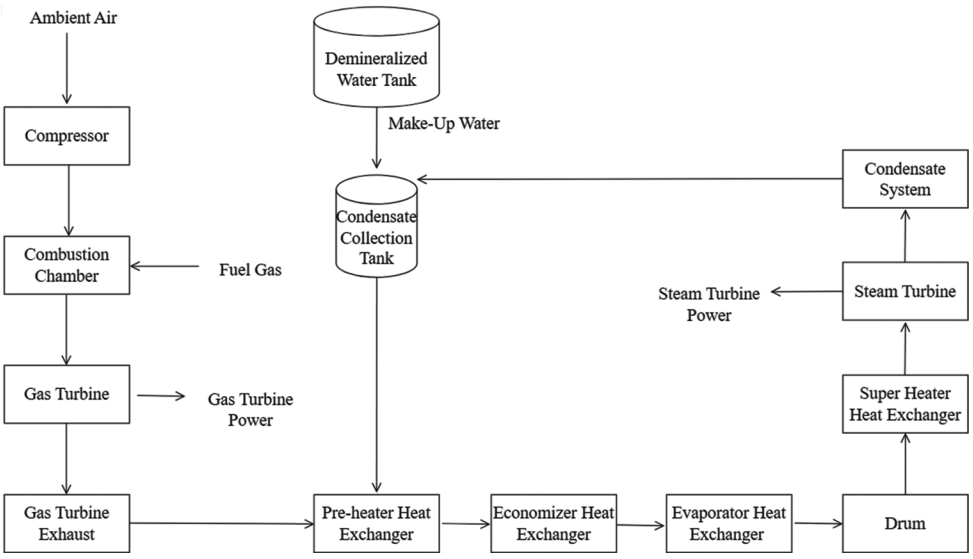

Fig. 1. Simplified block flow diagram of combined cycle gas turbine power plant.

case tractable, some assumptions were made, including: the CCGT system is assumed to run under steady-state circumstances; generalized corrected compressor maps are used; the simulated compressor is considered to be multistage; and no leakage of flue gas is considered from the HRSG blow-down. Based on these assumptions, the simulation work was separated into two main cases. Case 1 focused on simulating CCGT performance under part-load conditions using Aspen HYSYS data from (Liu and Karimi, 2018b), while Case 2 involved simulating CCGT part-load operation based on actual field data from Sulaymaniyah power plant (Sulaymaniyah CCGT Power Plant, 2022). This structured approach enables both comparative analysis with a well-established commercial simulator and validation against real operational behavior, thereby ensuring a more comprehensive and reliable assessment of CCGT performance under varying load conditions.

A. Case 1: Simulation of CCGT Power Plant Under Part-Load Operation Using Aspen HYSYS Data

The simulation of the GT is based on a general model described in previous work (Hassan and Manji, 2023). For Case 1 of the CCGT part-load operation, the process flow diagrams (PFDs) are presented in Fig. 2 for the GT, Fig. 3 for the combined cycle, and Fig. 4 for the ST. The design parameters used in the part-load equations and scenarios are summarized in Table I.

During part-load operation, the air filter is the first unit to be affected, with its performance reflected in the pressure drop across the filter. Under design conditions, the pressure drop of the air filter is very small, and it remains low even during part-load operation. The pressure drop can be calculated using Equation (1) (Liu and Karimi, 2018a), ensuring that variations in filter resistance are properly accounted for in the simulation and analysis of CCGT performance. Equation (1) is evaluated within the DWSIM spreadsheet, where the design variables are defined according to the parameters listed in Table I, while the variables that vary during part-load operation are directly imported from the DWSIM flowsheet. Once the pressure drop is calculated,

TABLE I
Design variable of CCGT Plant Case 1 (Liu and Karimi, 2018a)

Variable	Value
Ambient condition	
Pressure	1.013 bar
Temperature	15°C
Molar fraction	77.30% N_2, 20.74% O_2, 1.01% H_2O, 0.03% CO_2, 0.92% Ar
Fuel condition	
Pressure	30 bar
Temperature	10°C
Molar fraction	87.08% CH_4, 7.83% C_2H_6, 2.94% C_3H_8, 1.47% N_2, 0.68% CO_2
Gas turbine	
Inlet airflow	635 kg/s
Inlet air pressure loss	0.5 (%)
Compressor pressure ratio	15.4
Compressor isentropic efficiency	88%
Compressor mechanical efficiency	99%
Fuel flow	14.74 kg/s
Combustor efficiency	99.50%
Combustor pressure loss	3.50%
Combustor exit temperature	1405°C
Turbine inlet temperature	1328°C
Turbine exhaust temperature	615°C
Heat recovery steam generator (HRSG)	
HP/IP/LP steam temperatures	565.0/297.0/295°C
HP/IP/LP pinch point temperatures	10.0/10.0/10.0°C
HP/IP/LP approach point temperatures	8.0/10.0/16.4°C
HP Super-heated (SPHT 1) steam outlet temperature	510°C
RHT 1/2 steam outlet temperature	520.0/565.0°C
HP ECON 1/2 water outlet temperature	208.0/280.0°C
Pressure losses on gas/water/steam sides	1.5/5.0/3.0%
Steam turbines (STs)	
HP/IP/LP ST inlet pressure	98.8/24.0/4.0 bar
HP/IP/LP ST isentropic efficiency	87.0/91.0/89.0%
Shaft speed 3000	3000 rpm

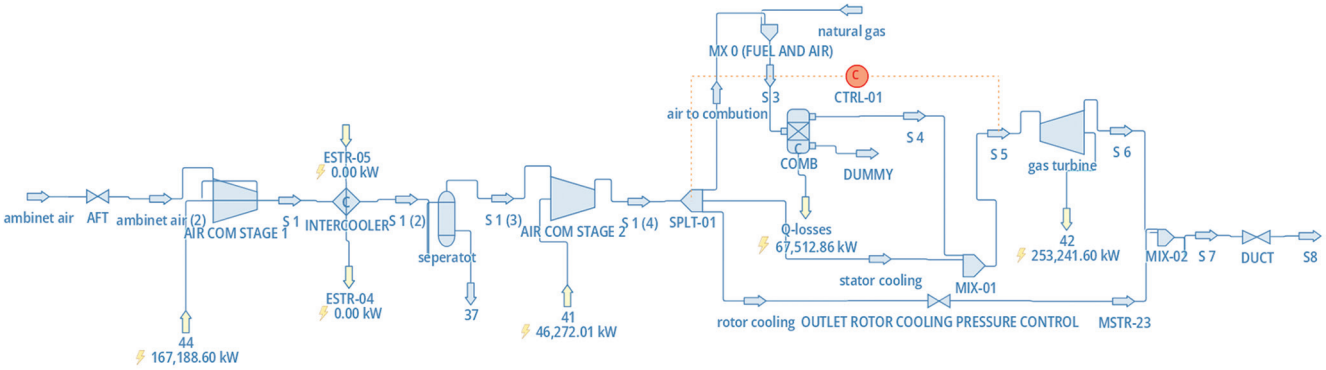

Fig. 2. Process flow diagram of the gas turbine for Case 1.

its value is exported back into the DWSIM flowsheet and assigned to the air filter of the turbine unit (AFT), which is modeled as an AFT valve. This integration ensures a dynamic link between the spreadsheet calculations and the simulation environment, allowing the pressure drop across the air filter to be continuously updated in response to part-load operating conditions.

$$\Delta P = \Delta P_d \left(\frac{m}{m_d}\right)^{1.84} \left(\frac{T}{T_d}\right) \left(\frac{P}{P_d}\right)^{-1} \tag{1}$$

According to the general methodology for a multistage compressor (Hassan and Manji, 2023), which divides the compressor into two stages with an intercooler connected by stream (S1), the pressure ratio changes for each stage are determined by Equations (2) and (3) (Sarathy, 2021). Where the intercooler outlet temperature is assumed not to change.

$$PR = \frac{P_2}{P_1} \tag{2}$$

$$P_r = \left[\frac{P_2}{P_1}\right]^{1/n} \tag{3}$$

The compressor mass flow is controlled by the IGV, whose opening and closing regulate the air entering the compressor. The IGV angle varies from 0% to 40%, where 0% corresponds to the IGV being fully open, and 40% indicates that the IGV is partially closed, reducing the plant load to 40% of its design capacity. Based on the IGV angle or the air mass flow rate, the appropriate performance curves can be selected in DWSIM.

As the air exits the multistage compressor, it is divided into three streams: one stream enters the combustion chamber for combustion, while the remaining two streams (stator and rotor) are used to control the GT inlet and outlet temperatures through mixer 1 (MIX1). The amount of cooling air required during part-load operation is estimated using Equation (4), which is implemented in the DWSIM spreadsheet.

$$m_{ca} = m_{ca,d} \left(\frac{P_{ca}}{P_{ca,d}}\right) \left(\frac{T_{ca,d}}{T_{ca}}\right)^{0.5} \tag{4}$$

The combustion chamber pressure drop is another parameter that changes during part-load operation. Equation (5)(Liu and Karimi, 2018b) was used to predict the combustion chamber pressure drop and has been implemented in the DWSIM spreadsheet.

$$\Delta P_{cc} = \Delta P_{cc,d} \left(\frac{m_{incc}\sqrt{T_{incc}}}{P_{incc}}\right)^2 / \left(\frac{m_{incc,d}\sqrt{T_{incc,d}}}{P_{incc,d}}\right)^2 \tag{5}$$

Using Equation (1), the pressure drops of the HRSG are calculated, added to the GT outlet pressure, and then exported as the duct pressure drop in DWSIM. Since the HRSG consists of a series of shell-and-tube heat exchangers, the heat transfer strongly depends on the hot flue gas mass flow. Consequently, the steam cycle is highly dependent on the GT flue gas mass flow, which is driven by the air compressor when the GT operates at partial load. Equation (6) describes the change in heat transfer during part-load operation in the heat exchangers (Liu and Karimi, 2018a).

$$UA = UA_d \left(\frac{m_g}{m_{g,d}}\right)^{0.8} \tag{6}$$

When the GT operates at part-load, its outlet temperature must be maintained at the design value to ensure proper HRSG operation. A cooling stream (stator and rotor) is used to regulate the GT outlet temperature. After all units of the CCGT are installed, the required amount of water from the low-pressure pump suction or condensate water (S64b) is fed into the cycle. Following preheating in the low-pressure (LP) economizer, the condensate water is split into three streams by SPLT3, which specifies the steam distribution leaving the LP, intermediate-pressure, and HP drums. Each stage then receives its required water, and controllers recycle (R) R7, R10, R5, R13, and R16 recalculate the water–vapor mixture needed in the boilers to generate the steam specified by SPLT3.

During part-load operation, R6 calculates the required water from SPLT2 to preheat the condensate water before it enters the LP economizer via RCP and MIX3. A trial-and-error approach is used to determine the correct condensate water amounts, ensuring the HRSG exhaust temperature remains near its design value and avoiding dewpoint formation in the exhaust. This strong dependency between GT exhaust flow and steam cycle performance is also highlighted in the work of Li, et al. (2017), where the HRSG

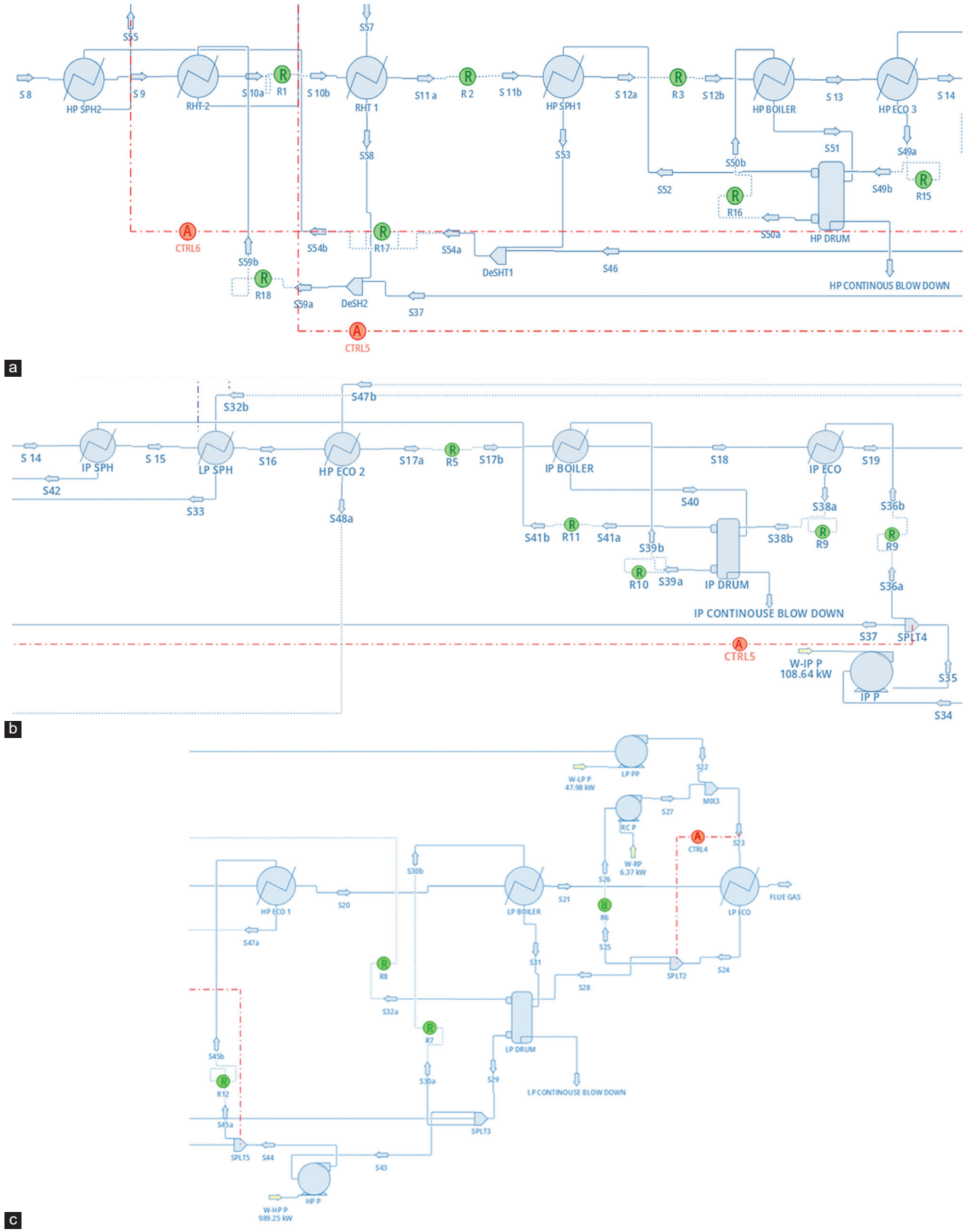

Fig. 3. Process flow diagram of the heat recovery steam generator for Case 1: (a) Upstream section, (b) intermediate section, and (c) downstream section. The complete PFD is provided in the Supplementary Material.

operation was shown to be directly influenced by variations in exhaust gas conditions. The present results further confirm the importance of maintaining a balance between exhaust flow and feedwater rate to ensure efficient heat recovery.

http://dx.doi.org/10.14500/aro.12620

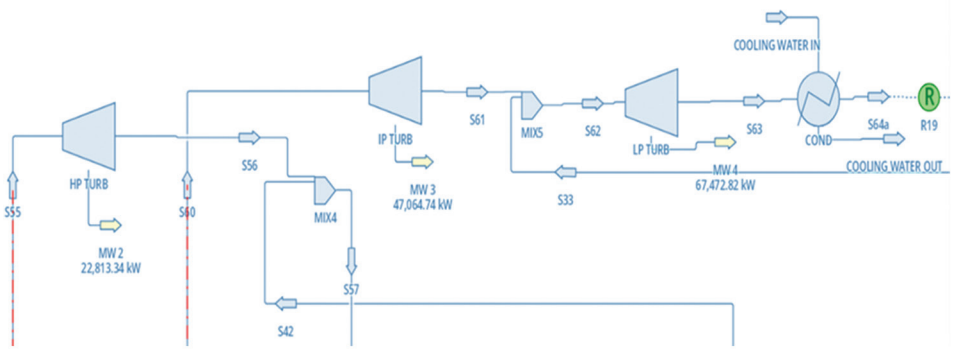

Fig. 4. Process flow diagram (PFD) of the steam turbine for Case 1, the complete PFD provided in the Supplementary Material.

As the GT exhaust mass flow decreases, the feedwater to the heat exchangers is reduced accordingly, maintaining a balance between the GT exhaust gas flow and the HRSG exhaust temperature. As the required super-heated steam is prepared from the heat exchanger, it enters the STs (Turb).

Overall, the results of Case 1 demonstrate strong agreement with both Aspen HYSYS simulations and previously published studies. The minor deviations observed can be attributed to modeling simplifications, such as intercooler temperature assumptions and differences in solver algorithms. Nevertheless, the trends in power output, efficiency, and mass flow behavior are consistent with the literature, confirming the reliability of DWSIM as an alternative simulation tool for CCGT performance analysis.

B. Case 2: Simulation of CCGT Power Plant under part-load operation using field Data (GT type F-9E manufactured by General Electric)

The PFD for part-load operation of CCGT Case 2 is shown in Fig. 2 for the GT, Fig. 5 for the combined cycle and HRSG, and Fig. 6 for the ST.

Case 2's simple cycle contains four GTs; in the proposed simulation, only one GT was simulated, while the others are assumed to operate under identical conditions. The multistage compressor pressure, calculated using Equations (2) and (3), is divided into two stages with an intercooler between them. Table II provides the design parameters used in the part-load equations and scenarios. The same strategy used in Case 1 for part-load operation was applied to Case 2, except different design parameter values as specified in Table II.

After storing the compressor maps in the DWSIM performance curve, Equation (4) is used to calculate the cooling air required for stator and rotor cooling, which varies during part-load operation. The combustion chamber pressure drop during part-load is predicted using Equation (5). The predicted HRSG pressure drop is calculated from Equation (1) and added to the GT outlet pressure. All these equations are implemented in the DWSIM spreadsheet and then exported to the appropriate units.

During part-load operation, GT power generation and exhaust temperature must be controlled, especially when integrated with the HRSG of a combined cycle ST. In this study, GT power was controlled by adjusting the compressor inlet air and fuel flow. The GT power output is reduced by decreasing the compressor air and fuel flow as needed, while maintaining the exhaust temperature at its design value.

All GTs are connected to the HRSG unit to generate high-pressure and high-temperature steam. The HRSG is simulated as two stages of steam pressure. The simulation is performed for only one HRSG, with the others assumed to operate under identical conditions. All superheated steam (HP and LP) conditions are simulated to produce the same amount of steam during part-load operation.

TABLE II
DESIGN VARIABLES OF THE CCGT PLANT FOR CASE 2

Variable	Value
Ambient condition	
Pressure	101.3 kPa
Temperature	13.3°C
Molar fraction	77.30% N_2, 20.74% O_2, 1.01% H_2O, 0.03% CO_2, 0.92% Ar
Fuel condition	
Pressure	23.8 bar
Temperature	40°C
Molar fraction	88.8% CH_4, 8.84% C_2H_6, 1.48% C_3H_8, 0.175% N_2, 0.093% CO_2
Gas turbine	
Inlet air flow	458.2 kg/s
Inlet air after pressure loss of filter house	0.82
Compressor pressure ratio	13
Compressor isentropic efficiency	91.10%
Fuel flow	6.9 kg/s
Combustor efficiency	99%
Combustor pressure loss	0.1
Combustor exit temperature	1390°C
Turbine inlet temperature	1050°C
Turbine exhaust temperature	547°C
Gas turbine thermal efficiency	32.20%
Heat recovery steam generator (HRSG)	
LP EVA outlet pressure	8.16 bar
HP EVA outlet pressure	72.8 bar
HP/LP steam temperatures	525.1/223.1 (°C)
HP SUPHT 1 steam outlet temperature	497.3 (°C)
HP ECON 1/2 water outlet temperature	120/284.2 (°C)
Steam turbines (STs)	turbines (STs)
HP/LP ST inlet pressure	67.15/6.04 (bar)
HP/LP ST isentropic efficiency	90/65 (%)
Shaft speed 3000	3000 (rpm)

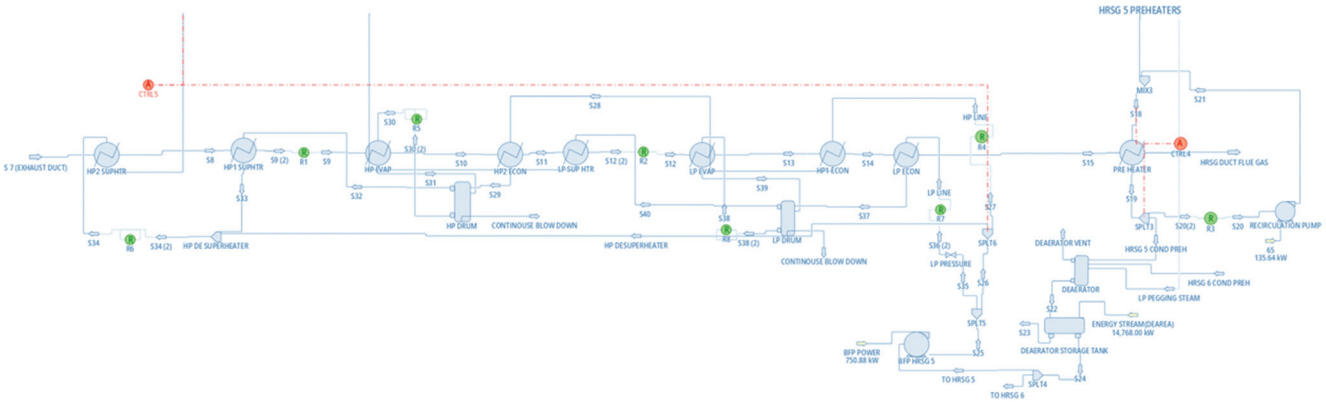

Fig. 5. Process flow diagrams (PFDs) of the combined cycle for Case 2 in DWSIM. The complete PFD provided in the Supplementary Material.

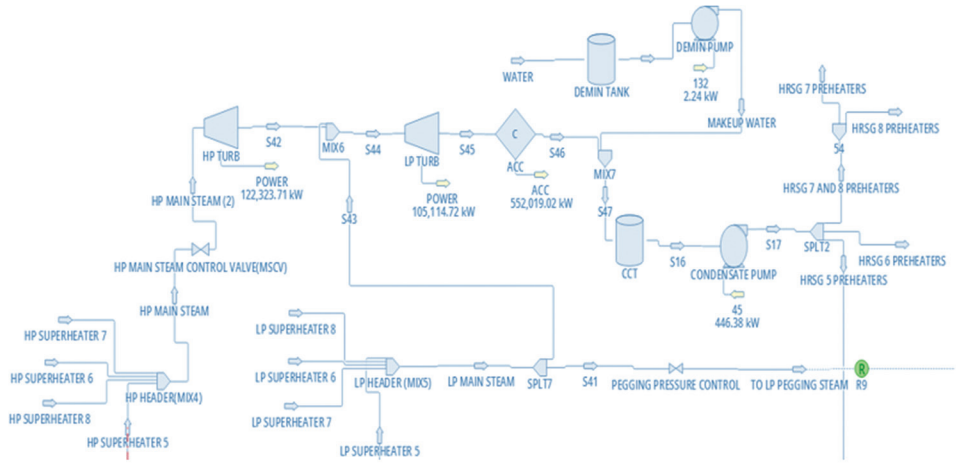

Fig. 6. Process flow diagram (PFD) of superheated main steam, steam turbines, and condensate system for Case 2 in DWSIM, the complete PFD provided in the Supplementary Material.

III. Results and Discussions

A. Case 1: Simulation Results using Aspen HYSYS Data

The validation of the Case 1 simulation results is carried out by comparing them with published data from the sources. During part-load operation, GT power output and exhaust temperature are the most critical parameters affecting CCGT plant performance and serve as the primary objectives of the cycle. Fig. 7 shows the deviations for the power generated in DWSIM with that produced in Aspen HYSYS for the GT during part-load operation, and Equation (7) is used to calculate the relative deviation (RD) between the two simulation models (Liu and Karimi, 2018b).

$$RD\ \% = \frac{DWSIM\ Result - ASPEN\ HYSYS\ Result}{ASPEN\ HYSYS\ Result} \times 100 \quad (7)$$

From Fig. 7, it can be observed that the power generation in DWSIM closely matches the Aspen HYSYS results across all plant load scenarios, with most relative deviations below 1%. The highest deviation occurs at 40% plant load, reaching 3.8%, where DWSIM GT power generation is slightly higher than the Aspen HYSYS result. This level of agreement is consistent with the findings of Liu and Karimi (2018b), who demonstrated that simulation-based models can reliably predict CCGT performance under part-load conditions when appropriate control strategies are implemented. The small deviation observed in this study, particularly at lower loads, may be attributed to differences in model assumptions and numerical implementation between DWSIM and Aspen HYSYS.

The GT exhaust temperature is a critical parameter during part-load operation, as it directly affects the steam cycle and must be maintained at the design value. Fig. 7 also illustrates the differences in GT exhaust temperature between DWSIM and Aspen HYSYS during part-load operation.

As shown in Fig. 7, the GT exhaust temperature was effectively controlled as designed. During part-load operation, the exhaust temperature for all plant loads was maintained at the design value of 615°C, with excellent agreement between the simulation results. Maintaining a constant exhaust temperature under part-load operation is a well-established control strategy in CCGT systems, as also reported by Xie, et al. (2024), where turbine control mechanisms were optimized to ensure stable HRSG performance. The results of this study confirm that DWSIM can effectively replicate this operational requirement.

GT compressors are highly sensitive to mass flow during part-load operation, as their outlet pressure and temperature

http://dx.doi.org/10.14500/aro.12620

are strongly influenced by it. Therefore, careful monitoring is required to achieve the desired power output and maintain the exhaust temperature.

Fig. 7 also compares the two simulation codes for mass flow rates, showing that they produce highly similar and plausible results up to 50% plant load. When the plant load drops below 50%, the DWSIM compressor requires lower mass flow rates to achieve the desired power and exhaust temperature. The relative deviation for plant loads above 50% remains small, not exceeding 4.4%.

Compressor operation and fuel flow jointly govern GT performance during part-load operation; therefore, any change in the IGV angle requires a corresponding adjustment in fuel flow, as both control the GT's power output and exhaust temperature. In addition, this figure shows that as the compressor mass flow decreases, the fuel flow also decreases. The comparison between the two models demonstrates close agreement. This coordinated reduction ensures that the exhaust temperature is maintained. This behavior is in agreement with previous studies (Encabo Caceres, Mocholí Montañés and Nord, 2018; Talah, Bentarzi and Mangola, 2023), which reported that both compressor mass flow rate and fuel flow must be simultaneously adjusted during part-load operation to maintain system stability and achieve the desired power output.

When the power demand decreases, the IGV reduces the compressor mass flow rate, and the fuel flow also decreases to produce the required power. Consequently, the GT inlet temperature fluctuates, as it is highly dependent on compressor performance and fuel flow. Fig. 7 shows the relative deviation between the used DWSIM models during part-load operation. The outputs are generally similar, with the highest deviation reaching - 9.8% at 45% plant load, where both compressor and fuel flow are low. This variation also arises from assuming the intercooler temperature equals the ambient temperature, which can be adjusted by modifying the air and fuel flows and the intercooler temperature through a trial-and-error approach.

In addition, as the GT power decreases, its efficiency also changes as clarified in Fig. 7, a reduction in plant load leads to a corresponding decrease in GT efficiency. The deviation between the two models during part-load operation is small, with the highest relative deviation reaching -4.36% for DWSIM when it is lower than the Aspen HYSYS value. The observed decrease in GT efficiency at part-load operation is consistent with thermodynamic expectations and has been widely reported in the literature (Encabo Caceres, Mocholí Montañés and Nord, 2018). This reduction is mainly due to off-design operation of the compressor and turbine, resulting in lower aerodynamic efficiency and increased irreversibilities.

Both the GT and the steam cycle operate under and are affected by part-load conditions. As the plant load varies, all processes adjust accordingly. The GT exhaust flow enters the HRSG duct without losses; therefore, when the GT exhaust flow decreases at lower plant loads, the steam cycle power generation also decreases, as shown in Fig. 7 when both simulators' results are very close. During part-load operation, ST power generation is governed by the condensate water flow, which interacts with the GT exhaust and HRSG. As the GT flue gas flow decreases, the condensate water must be reduced to prevent low temperatures in the HRSG exhaust duct and avoid dewpoint formation.

B. Case 2: Simulation Results using Field Data

Due to the limited availability of field data for part-load operation and the difficulty of observing plant behavior under fluctuating loads, the presented results cannot be directly compared with actual plant measurements. Figs. 8 and 9 illustrate how the compressor inlet air and fuel mass flow rates decrease in parallel with GT power output during part-load operation. These results demonstrate the reliability of DWSIM in simulating the GT cycle.

Similar trends have been reported in previous studies on part-load operation of GTs, where reductions in compressor inlet air and fuel flow were necessary to match lower power demands (Talah, Bentarzi and Mangola, 2023). This confirms that the simulation results follow realistic operational behavior.

Fig. 10 shows the GT inlet temperature during part-load operation. It illustrates that the GT inlet temperature decreases as power output decreases, helping to maintain the exhaust

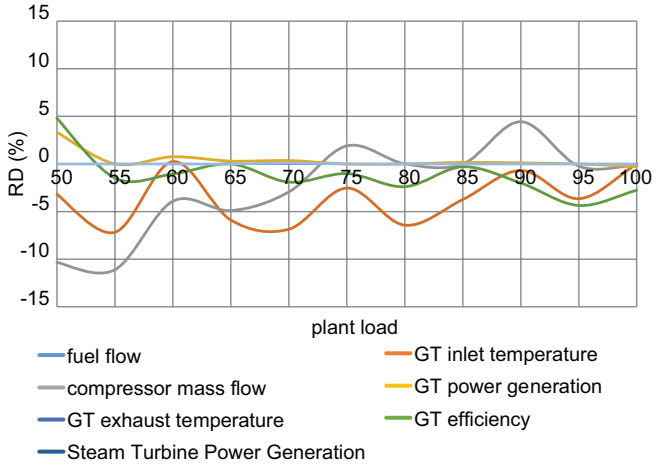

Fig. 7. Relative deviation of gas turbine parameters between DWSIM and aspen HYSYS under part-load operation.

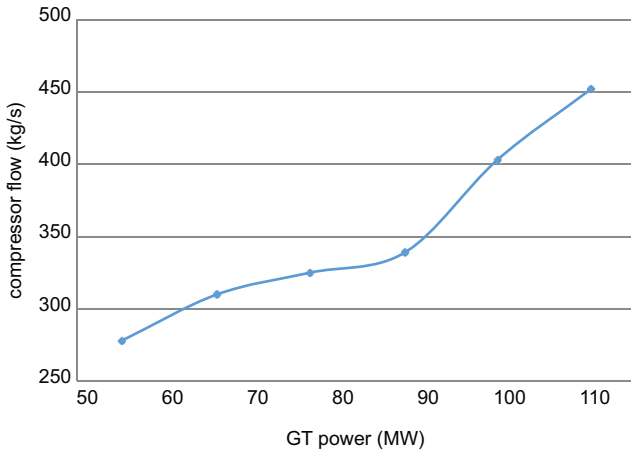

Fig. 8. Compressor inlet air mass flow rates versus gas turbine power.

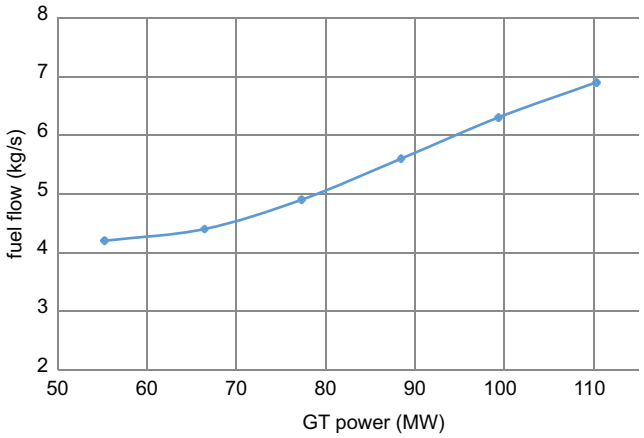

Fig. 9. Fuel mass flow versus gas turbine power.

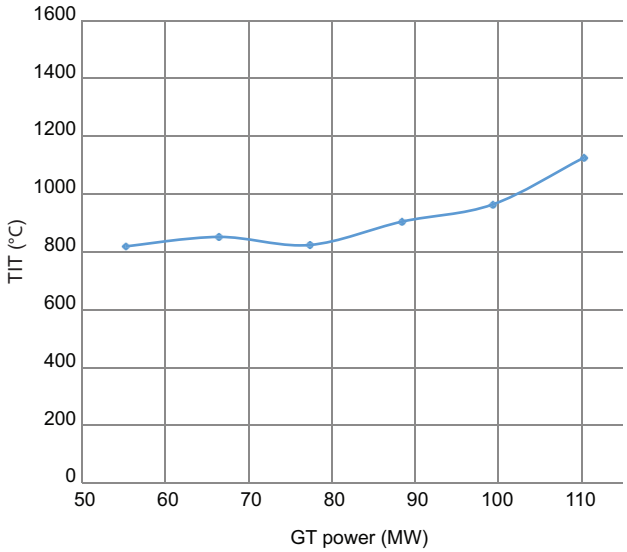

Fig. 10. Gas turbine (GT) inlet temperature versus GT power.

temperature at its design value. This trend is consistent with GT control strategies discussed in the literature, where turbine inlet temperature is adjusted alongside fuel flow to regulate power output while maintaining thermal limits (Xie, et al., 2024).

The GT exhaust temperature during part-load operation remains at the design value, confirming the effectiveness of GT control under part-load conditions.

As shown in Fig. 11, ST power generation is highly dependent on the GT exhaust flow. As GT power decreases, the exhaust flow rate also decreases, reducing the steam flow and, consequently, the ST power output. Fig. 12 illustrates how ST power generation declines in parallel with GT power during part-load operation. This proportional relationship between GT and ST power output has also been observed in previous CCGT studies (Li, et al., 2017), confirming that the bottoming cycle performance is highly dependent on the topping cycle conditions.

Fig. 12 shows that as GT power generation and its flue gas flow decrease, the condensate water flow in the steam cycle also decreases, resulting in reduced ST power generation.

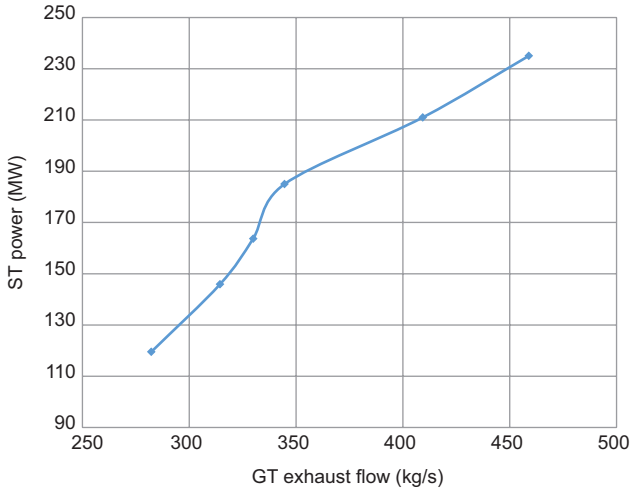

Fig. 11. Steam turbine power generation during part-load operation versus gas turbine exhaust flow.

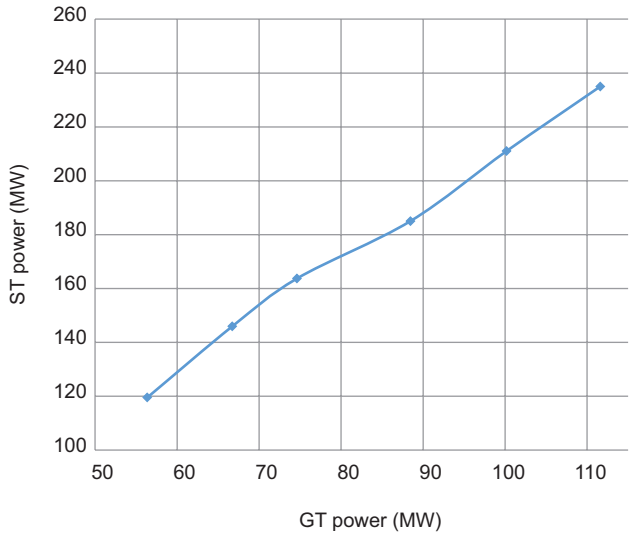

Fig. 12. Steam turbine power generation versus gas turbine power generation during part-load operation.

Meanwhile, the HRSG exhaust temperature during part-load operation is maintained above the NOx dew point. Figs. 12 and 13 demonstrate the excellent validation of using DWSIM to simulate HRSG and ST units.

Although direct validation with full field data was limited, the obtained trends are consistent with well-established thermodynamic principles and previously published simulation studies. A key contribution of this work is the use of actual plant data in combination with an open-source simulation tool, which is rarely addressed in the literature. This enhances the practical relevance of the study and demonstrates the applicability of DWSIM for real-world CCGT performance analysis.

In comparison with existing literature, most previous studies have relied on commercial simulation tools such as Aspen Plus, EBSILON, and Modelica environments for analyzing CCGT performance. The present study

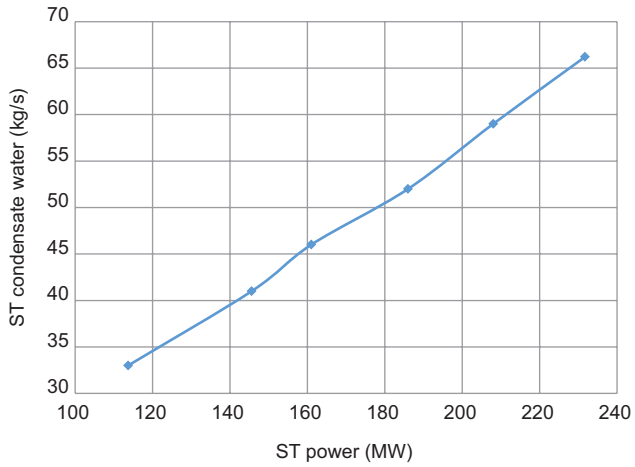

Fig. 13. Condensate water flow rates during steam turbine part-load operation.

demonstrates that DWSIM, as an open-source alternative, can achieve comparable accuracy in predicting part-load behavior. This finding aligns with recent studies (Ali Motamed, Genrup and Nord, 2024; Hashim, Hasan and Al Jubori, 2025), which highlighted the increasing capability of open-source tools in simulating complex energy systems. Furthermore, the integration of both literature-based validation (Case 1) and real field data (Case 2) provides a more comprehensive assessment than most previous works, representing a key contribution of this study.

IV. Conclusion

A careful simulation procedure was employed to model the CCGT power plant under part-load operation for two cases, with part-load equations successfully implemented in the DWSIM spreadsheet to control plant behavior. In Case 1, results closely matched Aspen HYSYS simulations, with minor differences, and GT power generation was nearly equivalent when the exhaust temperature was maintained at its design value, while accurately modeled HRSG units ensured adequate power and efficiency. In Case 2, the part-load strategy showed consistent reductions in compressor flow, fuel flow, GT outlet and inlet temperatures, and ST power as plant load decreased. These outcomes demonstrate that DWSIM can reliably simulate CCGT performance under a range of operating conditions, establishing it as a robust and dependable open-source tool for both design and part-load operation.

References

Ali Motamed, M., Genrup, M., and Nord, L.O., 2024. Part-load thermal efficiency enhancement in gas turbine combined cycles by exhaust gas recirculation. *Applied Thermal Engineering*, 244, p.122716.

Asadi, R., Assareh, E., Moltames, R., Olazar, M., Nedaei, M., and Parvaz, F., 2022. Optimisation of combined cooling, heating and power (CCHP) systems incorporating the solar and geothermal energy: A review study. *International Journal of Ambient Energy*, 43(1), pp.42-60.

Bass, R.J., Malalasekera, W., Willmot, P., and Versteeg, H.K., 2011. The impact of variable demand upon the performance of a combined cycle gas turbine (CCGT) power plant. *Energy*, 36(4), pp.1956-1965.

Boles, M., and Cengel, Y., 2014. *An Engineering Approach*. McGraw-Hill Education, New York.

Boyaghchi, F.A., Chavoshi, M., and Sabeti, V., 2015. Optimization of a novel combined cooling, heating and power cycle driven by geothermal and solar energies using the water/CuO (copper oxide) nanofluid. *Energy*, 91, pp.685-699.

Can Gülen, S., and Kim, K., 2014. Gas turbine combined cycle dynamic simulation: A physics based simple approach. *Journal of Engineering for Gas Turbines and Power*, 136(1), p.011601.

Csendes, V.F., Egedy, A., Leveneur, S., and Kummer, A., 2023. Application of multi-software engineering: A review and a kinetic parameter identification case study. *Processes*, 11(5), p.1503.

Dev, N., Samsher, Kachhwaha, S.S., and Mohit., 2012. Mathematical modeling and computer simulation of a combined cycle power plant. In: Deep, K., Nagar, A., Pant, M., Bansal, J. (eds) *Proceedings of the International Conference on Soft Computing for Problem Solving (SocProS 2011) December 20-22, 2011. Advances in Intelligent and Soft Computing*. Vol. 131. Springer, New Delhi.

Diddi, S., and Panda, S., 2024. *Implementing Simulation Software to Develop Virtual Experiments in Undergraduate Chemical Engineering Education*. Qeios. Available from: https://doi.org/10.32388/M3SNIJ [Last accessed on 2026 Jan 05].

Emenike, O.E., Anyaoha, C., and Okoroigwe, E.C., 2025. Energy analysis and optimization of open cycle gas turbine power plant through exhaust heat recovery. *NIPES-Journal of Science and Technology Research*, 7(3), pp.195-212.

Encabo Caceres, I., Mocholí Montañés, R., and Nord, L.O., 2018. Flexible operation of combined cycle gas turbine power plants with supplementary firing. *Journal of Power Technologies*, 98(9), pp.188-197.

Glazar, V., Mrzljak, V., and Gubic, T., 2019. Thermodynamic analysis of combined cycle power plant. In: *14th International Conference Heat Transfer, Fluid Mechanics and Thermodynamics*. pp.341-355.

Hashim, S.A., Hasan, M.R., and Al Jubori, A.M., 2025. Performance evaluation of a combined gas turbine power cycle and absorption chiller in design and off-design operation under different control strategies. *Engineering, Technology* and *Applied Science Research*, 15(4), pp.24226-24235.

Hassan, T.N., and Manji, S.T., 2023. Simulating combined cycle and gas turbine power plant under design condition using open-source software DWSIM: A comparative study. *ARO-The Scientific Journal of Koya University*, 11(1), pp.60-71.

Hussein, H.M.M., and İbrahim, S.A.A.S., 2024. Thermodynamic and Thermoeconomic Optimization of Combined Cycle Gas Turbine Power Plants for Enhanced Efficiency. In: *2024 8th International Symposium on Multidisciplinary Studies and Innovative Technologies (ISMSIT)*. pp1-13.

Ibrahim, T.K., Kamil, M., Awad, O.I., Rahman, M.M., Najafi, G., Basrawi, F., Abd Alla, A.N., and Mamat, R., 2017. The optimum performance of the combined cycle power plant: A comprehensive review. *Renewable and Sustainable Energy Reviews*, 79, pp.459-474.

Ibrahim, T.K., and Rahman, M.M., 2015. Optimum performance improvements of the combined cycle based on an intercooler–reheated gas turbine. *Journal of Energy Resources Technology*, 137(6), p.061601.

Jeffs, E., 2008. *Generating Power at High Efficiency: Combined Cycle Technology for Sustainable Energy Production*. Elsevier, Amsterdam.

Khan, M.S., Xuebing, P., Yuntao, S., Bin, G., and Imran, M., 2024. An optimization of efficient combined cycle power generation system for fusion power reactor. *Case Studies in Thermal Engineering*, 57, p.104344.

Kong, Z.Y., Omar, A.A., Lau, S.L., and Sunarso, J., 2024. Introducing process simulation as an alternative to laboratory session in undergraduate chemical engineering thermodynamics course: A case study from Sunway University Malaysia. *Digital Chemical Engineering*, 12, p.100167.

Leisen, R., Radek, J., and Weber, C., 2024. Modeling combined-cycle power plants in a detailed electricity market model. *Energy*, 298, p.131246.

Li, D., Hu, Y., He, W., and Wang, J., 2017. Dynamic modelling and simulation of a combined-cycle power plant integration with thermal energy storage. In: *2017 23rd International Conference on Automation and Computing (ICAC)*. pp.1-6.

Liu, Z., and Karimi, I.A., 2018a. Simulating combined cycle gas turbine power plants in Aspen HYSYS. *Energy Conversion and Management*, 171, pp.1213-1225.

Liu, Z., and Karimi, I.A., 2018b. Simulation and optimization of a combined cycle gas turbine power plant under part-load operation. *Computer Aided Chemical Engineering*, 44, pp.2401-2406.

Lu, N., Pan, L., Pedersen, S., Zhang, D., and Arabkoohsar, A., 2024. A complete dynamic modeling of two-by-one gas-steam combined cycle unit for coordinated control design. *Applied Thermal Engineering*, 253, p.123766.

Meegahapola, L., and Flynn, D., 2014. Gas turbine modelling for power system dynamic simulation studies. In: Gonzalez-Longatt, F.M., and Luis Rueda, J., (Eds.), *Power Factory Applications for Power System Analysis*. Springer International Publishing, Berlin. pp.175-195.

Najjar, Y.S.H., and Akyurt, M., 1994. Combined cycles with gas turbine engines. *Heat Recovery Systems and CHP*, 14(2), pp.93-103.

Ohanu, C.P., Rufai, S.A., and Oluchi, U.C., 2024. A comprehensive review of recent developments in smart grid through renewable energy resources integration. *Heliyon*, 10(3), e25705.

Pal, S.K., Laukkanen, T., Saeed, L., Järvinen, M., and Karlsson, V., 2015. Simulation and analysis of a combined cycle heat and power plant process. *International Journal of Sustainable Engineering*, 8(4-5), pp.268-279.

Pan, M., Aziz, F., Li, B., Perry, S., Zhang, N., Bulatov, I., and Smith, R., 2016. Application of optimal design methodologies in retrofitting natural gas combined cycle power plants with CO2 capture. *Applied Energy*, 161, pp.695-706.

Pattanayak, L., Padhi, B.N., and Gajjar, H., 2021. Thermodynamic Modeling and Performance Simulation of Combined Cycle Power Plant Under Design and Off-Design Condition. In: *Gas Turbine India Conference*, *85536*, V001T12A001.

Ravelli, S., 2025. The role of part-load control strategies in optimizing the efficiency of a decarbonized combined cycle power plant in load-following mode. *Journal of Engineering for Gas Turbines and Power*, 147(12), p.121002.

Sadeghi, S., and Ahmadi, P., 2021. Thermo-economic optimization of a high-performance CCHP system integrated with compressed air energy storage (CAES) and carbon dioxide ejector cooling system. *Sustainable Energy Technologies and Assessments*, 45, p.101112.

Sarathy, J.V., 2021. Gas compression stages-design and optimization. *Engineering Practice Magazine*, 8(24), pp.15-18.

Sulaymaniyah CCGT Power Plant., 2022. Sulaymaniyah Combine Cycle PowerPlant. Mass Company, Sulaymaniyah, Iraq.

Talah, D., Bentarzi, H., and Mangola, G., 2023. Modeling and simulation of an operating gas turbine using Modelica language. *Revue Roumaine Des Sciences Techniques-Série Électrotechnique Et Énergétique*, 68(1), pp.102-107.

Xezonakis, V., Samuel, O.D., and Enweremadu, C.C., 2024. Modelling and output power estimation of a combined gas plant and a combined cycle plant using an artificial neural network approach. *Journal of Engineering*, 2024(1), p.5540010.

Xie, Q., Wu, H., and Deng, L.P., 2024. Improving part-load performance of combined-cycle gas turbines by optimizing variable geometry control strategy for compressor and power turbine combined adjustment. *Proceedings of the Institution of Mechanical Engineers, Part A: Journal of Power and Energy*, 238(7), pp.1197-1212.

Xu, Q., Li, X., Yu, J., Wang, S., Luo, K., and Fan, J., 2024. Optimization of parameters and thermodynamics of gasification process for enhanced CO_2 capture in an IGCC system. *Energy*, 304, p.131853.

Zabre, E., Roldan-Villasana, E.J., Romero-Jiménez, G., and Cruz, R., 2009. *World Congress on Engineering and Computer Science: WCECS 2009*.

http://dx.doi.org/10.14500/aro.12620

Supplementary Material

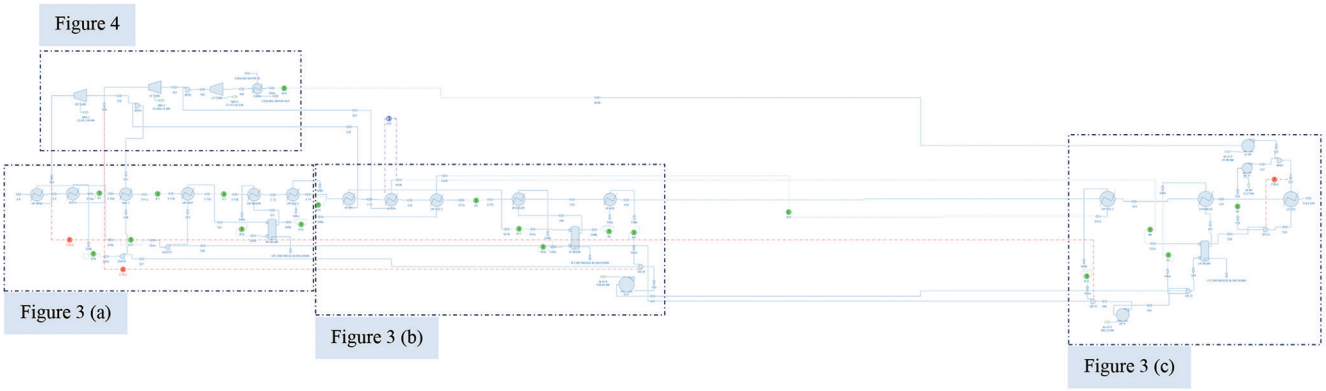

Supplementary material Fig. 3 and 4.

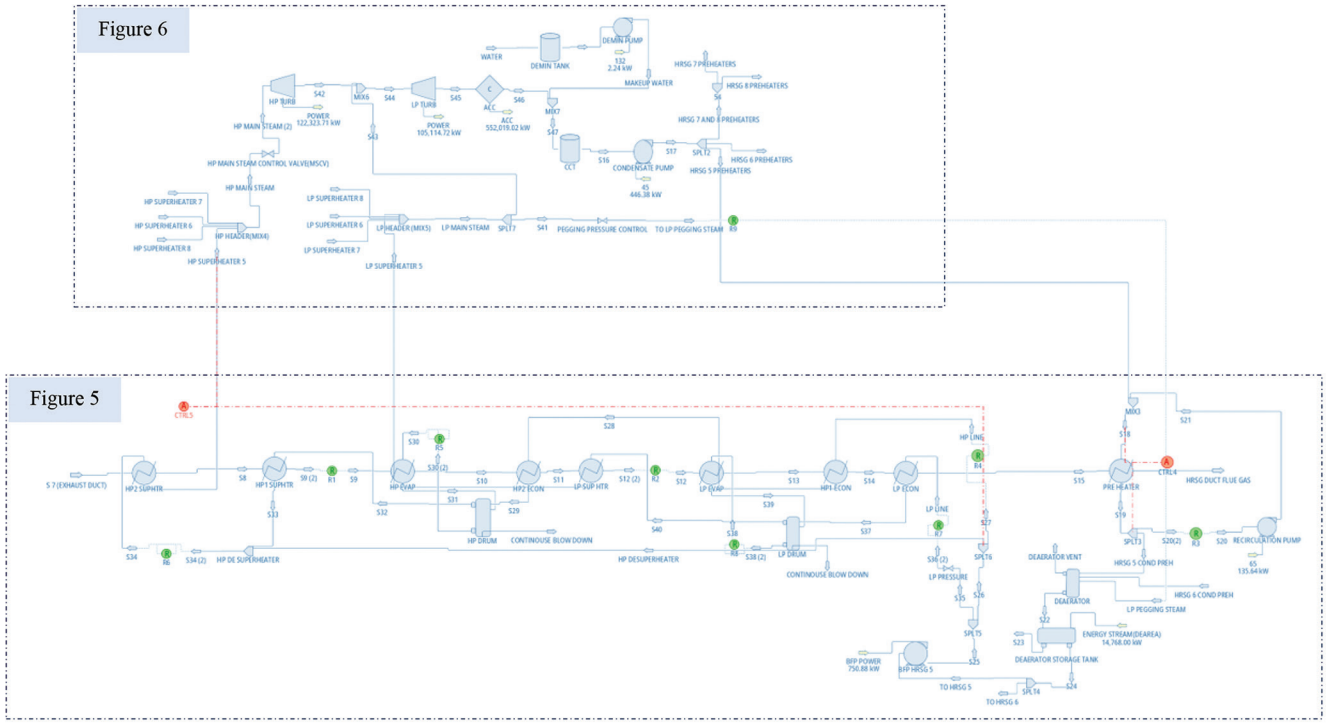

Supplementary material Fig. 5 and 6.